AIMS Mathematics

http://www.aimspress.com/journal/Math

AIMS Mathematics, 9(5): 12433–12457.
DOI: 10.3934/math.2024608
Received: 22 February 2024
Accepted: 21 March 2024
Published: 29 March 2024

Research article

Stochastic epidemic model for the dynamics of novel coronavirus transmission

Tahir Khan[1], Fathalla A. Rihan[1,*], Muhammad Bilal Riaz[2,3,*], Mohamed Altanji[4], Abdullah A. Zaagan[5] and Hijaz Ahmad[6,7,8]

[1] Department of Mathematical Sciences, UAE University, Al-Ain, P.O. Box 15551, United Arab Emirates

[2] IT4Innovations, VSB – Technical University of Ostrava, Ostrava, Czech Republic

[3] Department of Computer Science and Mathematics, Lebanese American University, Byblos, Lebanon

[4] Department of Mathematics, College of Science, King Khalid University, Abha, 61413, Saudi Arabia

[5] Department of Mathematics, Faculty of Science, Jazan University, P.O. Box 2097, Jazan 45142, Saudi Arabia

[6] Department of Mathematics, Faculty of Science, Islamic University of Madinah, Medina 42210, Saudi Arabia

[7] Center for Applied Mathematics and Bioinformatics, Gulf University for Science and Technology, Mishref, Kuwait

[8] Near East University, Operational Research Center in Healthcare, TRNC Mersin 10, Nicosia, 99138, Turkey

* **Correspondence:** Email: frihan@uaeu.ac.ae, muhammad.bilal.riaz@vsb.cz.

Abstract: Stochastic differential equation models are important and provide more valuable outputs to examine the dynamics of SARS-CoV-2 virus transmission than traditional models. SARS-CoV-2 virus transmission is a contagious respiratory disease that produces asymptomatically and symptomatically infected individuals who are susceptible to multiple infections. This work was purposed to introduce an epidemiological model to represent the temporal dynamics of SARS-CoV-2 virus transmission through the use of stochastic differential equations. First, we formulated the model and derived the well-posedness to show that the proposed epidemiological problem is biologically and mathematically feasible. We then calculated the stochastic reproductive parameters for the proposed stochastic epidemiological model and analyzed the model extinction and persistence. Using the stochastic reproductive parameters, we derived the condition for disease extinction and persistence. Applying

these conditions, we have performed large-scale numerical simulations to visualize the asymptotic analysis of the model and show the effectiveness of the results derived.

Keywords: stochastic differential equations; existence analysis; Itô formula; Lyapunov function; extinction; persistence; Milstein's higher order scheme; numerical simulations
Mathematics Subject Classification: 26A33, 34A08, 34A12

1. Introduction

The emergence of the severe acute respiratory syndrome coronavirus 2 (SARS-CoV-2) in late 2019 has caused unprecedented problems in health around the globe. The infection of the novel coronavirus has led to a devastating loss of lives and the production of a substantial burden on healthcare systems around the worldwide. Due to its urgency, the scientific community wants to comprehend the complexity of the disease and has hence investigated the spreading of SARS-CoV-2 not only by symptomatic individuals, but also by those who exhibited no apparent signs of illness but still transmitted the disease to others, i.e., asymptomatic individuals [1]. Symptomatic individuals experience cough, fever, and other respiratory symptoms which are recognized as the primary sources of disease transmission. The role of asymptomatic individuals has been gaining increasing amounts of attention because these individuals with no symptoms can transmit the disease to others making it difficult to control the spread of the novel coronavirus. Scholars have previously noted that 47% and 38% of newly infected cases are reported to be due to the contact with asymptomatic and symptomatic individuals, respectively [2]. Therefore, the existence of a small number of asymptomatic populations can produce a major disaster. The identification and understanding of the dynamics of both asymptomatic and symptomatic individuals can help to control the novel infection with the aid of effective control mechanisms.

Modeling the epidemiological process is a useful tool and has been vastly utilized to test various theories related to the dynamics and control of communicable diseases [3–6]. Different researchers have used these models to investigate the temporal dynamics of infectious diseases [7–13]. Dynamical systems representing the SARS-CoV-2 virus transmission are also abundant in literature, and numerous epidemiological models have been frequently exercised to investigate the predictability of the disease spread; see for instance [14–17]. Indeed, the models reported to represent the temporal dynamics of the novel coronavirus yielded interesting results; however, the authors mostly used a deterministic approach to model the interacting components of the novel model of coronavirus spread. Disease transmission is different everywhere due to the environment of the area and the immune system of the individual as well as the death rate and implementation of the vaccination program varying from place to place. Thus, due to the complex nature of SARS-CoV-2, it is observed that the novel disease has a stochastic nature. Recently, a model utilizing a stochastic approach has been studied to investigate the dynamics of coronavirus 2, as detailed in [18], where the authors did not consider various important factors that greatly influence the disease dynamics, e.g., the classification of infected individuals as a symptomatic and asymptomatic individuals has not been considered. However, models with an appropriate structure provide accurate dynamics and forecast the long-term spread for the disease which is very helpful for public health officials. Thus, we have formulated an epidemiological model

by taking the extended version of the model reported in [18] to represent the accurate dynamics of the novel coronavirus and realize the following contributions:

- Infected individuals are included as asymptomatic and symptomatic individuals because they are very important in the pandemic trend of the SARS-CoV-2 virus transmission. In fact, the existence of asymptomatic individuals with a small amount of the virus can create a major outbreak because without experiencing any symptoms, they produce environmental reservoirs and transmit the disease to others.
- We have investigated the multi-infection pattern of the novel of coronavirus by applying various phases of asymptomatic and symptomatic, and we show that successful interaction between the susceptible population and infected individuals either leads to symptomatic or asymptomatic individuals; therefore, have applied probability-based transmission while applying the outflow of the susceptible population to either infected group of individuals.
- The randomness is taken in each group of the model compartments because every parameter involved in the epidemic process of the novel coronavirus disease has a stochastic nature.
- We have developed an algorithm for the model simulations by using Milstein's higher order procedure to check the validity of the analytical work and represent the long-term with the aid of numerical simulations.

Thus, the goal of this study was to explore the dynamics of novel coronavirus transmission by including the above features and enhancing the model by taking an extended version of the model studied in [18]. To this end, we chose to classify the various infected sources of disease transmission as symptomatic, asymptomatic, and environmental reservoirs, and to take the randomness in every group of individuals by using different Brownian motions according to the disease characteristics. Keeping in view these hypotheses, we chose to first formulate the model and discuss its feasibility in the form of existence analysis and positivity. For this, we will use a combination of the Itô formula and the Lyapunov function. We then calculate the various stochastic reproductive parameters to discuss the conditions for the persistence and extinction of the novel coronavirus. In addition, we discuss the detailed extinction and persistence analysis of the model and derived sufficient conditions for it in terms of the stochastic reproductive parameters. Finally, to interpret the obtained results based on graphical visualization, we chose to develop an algorithm by using the Milstein higher-order method and present the large-scale numerical simulations of the model.

To provide a comprehensive and systematic analysis of the paper, we present the organization of the paper as follows. Following the introduction and recent literature, we formulate the model with a complete description in Section 2. To show the feasibility of the epidemic problem, we provide some basic concepts and notations and discuss the model analysis in Section 3. Subsequently, to examine the model extinction and persistence, and to derive sufficient conditions for it, we investigate the extinction and persistence analysis in Section 4. In addition, to perform the large-scale numerical simulations of the model, we have developed the algorithm by using of Milstein's Higher Order method, as presented in Section 5. Particularly, the discretization of the model is reported in Section 5.1, while the numerical experiments are presented in Section 5.2. Lastly, we conclude the summary of our work with the main findings in Section 6.

2. The model structure

In this part, we formulated the model for the dynamics of the novel coronavirus transmission keeping in view the characteristics of latent/asymptomatic and symptomatic individuals, as well as the environmental reservoirs. We assume that $(\Theta, Q_T, (Q_t)_{t\in[0,T]}, P)$ is a space of filtered probability that includes a 5D-Brownian motion $W := (W(t))_{t\geq 0}$, where $W(t) := (W_1(t), W_2(t), W_3(t), W_4(t), W_5(t))$. The novel disease transmits via environmental reservoirs and human interaction, differing everywhere. We, therefore, assume that groups of the model population will have a stochastic nature that is driven by different randomness sources i.e., $W_i(t)$, $i = 1, \ldots, 5$. The proposed epidemiological model incorporates the variations in all groups of individuals associated with various sources of information denoted by $Q = (Q_t)_{t\geq 0}$, where $Q_t := \sigma(W(t))$ represents the $\sigma-$algebra derived from $W(t)$; thus, the fluctuations are considered to be taken in all groups of individuals in the model. Further, the groups of humans are categorized into susceptible, latent or asymptomatic, symptomatic, and recovered groups, which are respectively denoted by $S(t)$, $L(t)$, $B(t)$, and $R(t)$, while the concentration of environmental reservoirs is symbolized by $C(t)$. In addition, we provided the flow diagram that represents the transfer mechanism for the model population in Figure 1.

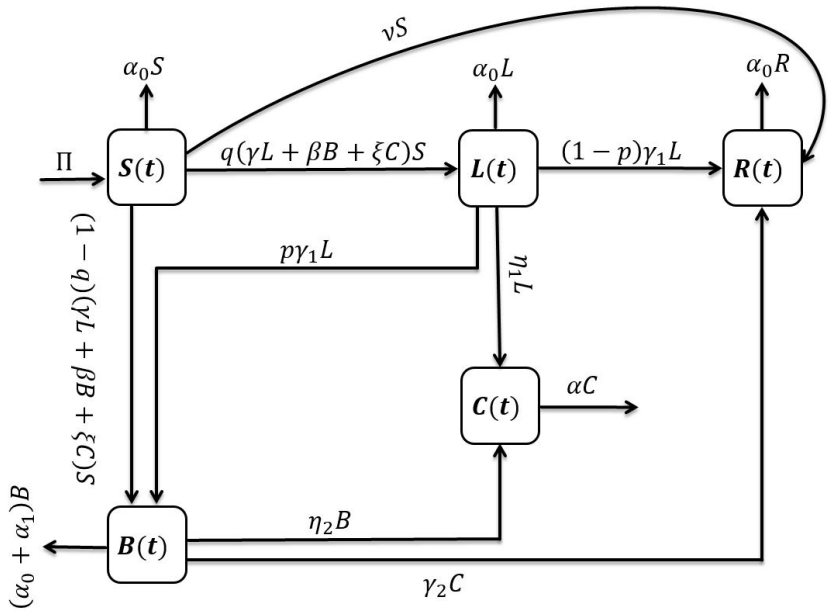

Figure 1. The plot represents the flow diagram of the proposed model.

Thus, the below dynamical system represents the novel coronavirus dynamics:

$$\begin{aligned}
dS(t) &= \{\Pi - \gamma L(t)S(t) - \beta S(t)B(t) - \xi S(t)C(t) - (\alpha_0 + v)S(t)\}\,dt \\
&\quad + \vartheta_1 S(t)dW_1(t), \\
dL(t) &= \{q(\gamma L(t)S(t) + \beta S(t)B(t) + \xi S(t)C(t)) - (\alpha_0 + \gamma_1)L(t)\}\,dt \\
&\quad + \vartheta_2 L(t)dW_2(t), \\
dB(t) &= \{(1-q)(\gamma L(t)S(t) + \beta S(t)B(t) + \xi S(t)C(t)) + p\gamma_1 L(t) \\
&\quad - (\alpha_1 + \gamma_2 + \alpha_0)B(t)\}dt + \vartheta_3 B(t)dW_3(t), \\
dR(t) &= \{\gamma_1(1-p)L(t) + \gamma_2 B(t) + vS(t) - \alpha_0 R(t)\}\,dt + \vartheta_4 R(t)dW_4(t), \\
dC(t) &= \{\eta_1 L(t) + \eta_2 B(t) - \alpha C(t)\}\,dt + \vartheta_5 W(t)dW_5(t).
\end{aligned} \tag{2.1}$$

In the model (2.1), the rate of births is denoted by Π, while the parameters γ, β, and ξ are used to represent the disease transmission from various sources. Vaccination for the novel coronavirus plays a significant role and it denoted by v, while α_0 denotes the natural death rate. Moreover, the death rate attributable to the novel disease is described by α_1, and p is the probability of direct recovery of latent/asymptomatic individuals, as some individuals directly recover without producing any symptoms. We also use q as the probability at which the susceptible individuals enter the asymptomatic/latent population, and γ_1 and γ_2 are the portions of individuals who recover from the contagious infection of the novel coronavirus disease. In addition, $W_i(t)$ and ϑ_i, $i = 1, \ldots, 5$ are the standard Brownian motions and white noise intensities, respectively, satisfying that $W_i(0) = 0$ and $\vartheta_i^2 > 0$ for all $i = 1, 2, 3, 4, 5$.

3. The analysis of the model

In this part, we show the model feasibility to prove the well-posedness of the proposed epidemic model. Particularly, we discuss the existence analysis of the model and its positivity. However, before presenting the results, first, we briefly recall some basic concepts that are helpful for deriving our conclusion.

Lemma 3.1. *[19] Let $u = (u_1, u_2, \ldots, u_k)$ and $v = (v_1, v_2, \ldots, v_k)$ represent two square-integrable adopted processes with k-dimensions. We assume the process $Y = (y_1, y_2, \ldots, y_k)$ for $n \in \{1, 2, 3, \ldots, k\}$; then, Y_n is expressed as the following differential equation:*

$$dY_n = u_n(t)dt + v_n(t)dW(t), \quad Y_n(0) \in \mathcal{R}. \tag{3.1}$$

If a function G from $\mathcal{R}^k$ to R is twice continuously differentiable, then

$$dG = \sum_{n=1}^{k} \frac{\partial G}{\partial x_n} dY_n(t) + \sum_{n,m=1}^{k} \frac{1}{2} \frac{\partial^2 G}{\partial x_n \partial x_m} \langle dY_n, dY_m \rangle, \tag{3.2}$$

where $\langle , \rangle$ represents the quadratic variation; therefore, $\langle dW(t), dW(t) \rangle = dt$ and $\langle dt, dW(t) \rangle = \langle dW(t), dt \rangle = \langle dt, dt \rangle = 0$.

In addition, to examine the extinction and persistence with the aid of the proposed model, we first describe the definitions that will be used in the model extinction and persistence analysis. Let

$$\langle \mathcal{P}(t) \rangle = \frac{1}{t} \int_0^t \mathcal{P}(a) da. \tag{3.3}$$

Then, the disease persists if $\lim(\inf\langle L(t)\rangle)$, $\lim(\inf\langle B(t)\rangle)$ and $\lim(\inf\langle C(t)\rangle)$ are positive whenever t increases without bound or equivalently, we can say that the epidemiological model (2.1) persists if

$$\liminf_{t\to\infty} \int_0^t L(a)da, \quad \liminf_{t\to\infty} \int_0^t B(a)da, \quad \liminf_{t\to\infty} \int_0^t C(a)da, \tag{3.4}$$

are positive.

Moreover, we assume that $\mathcal{R}_a^S$, $\mathcal{R}_b^S$, $\mathcal{R}_c^S$, and $\mathcal{R}_d^S$ are the components of the stochastic reproductive parameter, and they are respectively defined by

$$\begin{aligned} \mathcal{R}_a^S &= \frac{q\{\gamma+\beta+\xi\}\Pi}{\{\alpha_0+\nu\}\left\{\alpha_0+\gamma_1+\frac{\vartheta_2^2}{2}\right\}}, \quad \mathcal{R}_b^S = \frac{(1-q)\{\gamma+\beta+\xi\}\Pi}{\{\alpha_0+\nu\}\left\{\alpha_0+\alpha_1+\gamma_2+\frac{\vartheta_3^2}{2}\right\}}, \\ \mathcal{R}_c^S &= \frac{q\gamma\Pi}{\{\alpha_0+\nu\}\left\{\alpha_0+\gamma_1+\frac{\vartheta_2^2}{2}\right\}}, \quad \mathcal{R}_d^S = \frac{(1-q)\beta\Pi}{\{\alpha_0+\nu\}\left\{\alpha_0+\alpha_1+\gamma_2+\frac{\vartheta_3^2}{2}\right\}}. \end{aligned} \tag{3.5}$$

Then, the stochastic reproductive parameter for the epidemiological model (2.1) becomes $\mathcal{R}_0^S = \mathcal{R}_a^S + \mathcal{R}_b^S + \mathcal{R}_c^S + \mathcal{R}_d^S$.

In order to show the model existence analysis, we use a combination of the Itô formula and Lyapunov theory. Define

$$\Phi = \left\{(S,L,B,R,C) \in \mathcal{R}_+^5 \;\; S,R>0,\; A,B,C \geq 0,\; S+L+B+R+C \leq 1\right\}. \tag{3.6}$$

Thus, regarding the model existence the result will be shown in the following theorem.

Theorem 3.2. *For the initial conditions* $(S(0),L(0),B(0),R(0),C(0))$ *contained in* $\mathcal{R}_+^5$*, there exists a solution* $(S(t),L(t),B(t),R(t),C(t))$ *of the epidemiological model (2.1) which is unique and remains in* $\mathcal{R}_+^5$ *such that*

$$p\{(S,L,B,R,C) \in \Phi, \quad \forall \quad t \geq 0\} = 1.$$

Proof. Noted that for the model that is under consideration, the local Lipschitz continuity condition holds by following the methodology as adopted by Lei and Yang in [20]. Let $X = (S,L,B,R,C)$ be the model solution for all t in $[0,t_e)$ (where t_e is the explosion time), while X_0 symbolizes the initial values $(S(0),L(0),B(0),R(0),C(0))$ for the model contained in $\mathcal{R}_+^5$; then, the property of Lipschitz continuity implies that the solution of the model (2.1) is unique and local. To demonstrate that the solution is global, it is enough to show that $t_e = \infty$. To proceed further, we assume a constant $\varrho_0 \geq 0$ that is sufficiently large apply $\frac{1}{\varrho_0} < X_0 < \varrho_0$ and define the stopping time as follows:

$$t_\varrho = \inf\left\{t \in [0,t_e) : \min X \leq \frac{1}{\varrho} \text{ or } \max X\right\}. \tag{3.7}$$

Note that $\inf \varphi = \infty$, where φ represents the null set; also, since t_ρ varies with changing ϱ, that is if ϱ increases without bound, t_ϱ also increases. For $t \to \infty$, we set $\lim = t_\infty$ and $t_\infty = \infty$. Thus, we need to prove that $t_e = \infty$ only. Let $0 < \zeta < 1$, $T > 0$, and

$$P\{t_\infty \leq T\} > \zeta. \tag{3.8}$$

For $\varrho_1 \geq \varrho_0$

$$P\{t_\varrho \leq T\} \geq \zeta, \quad \text{for every} \quad \varrho \geq \varrho_1. \tag{3.9}$$

Let $\mathcal{H}$ contained in C^2 such that $\mathcal{H} : \mathcal{R}_+^5 \to \mathcal{R}_+$ be defined by

$$\mathcal{H} = L - \log(L) - 1 + B - \log(B) - 1 + S - \log(S) - 1 + R - 1 - \log(R) + C - \log(C) - 1. \tag{3.10}$$

Note that $\mathcal{H} \geq 0$; thus, for $\varrho_0 \leq \varrho$ and $T \geq 0$, the implementation of the Itô formula yields

$$\begin{aligned} d\mathcal{H} = U\mathcal{H}dt + \vartheta_1(S-1)dW_1 + (L-1)\vartheta_2 dW_2 + (B-1)\vartheta_3 dW_3 \\ + \vartheta_4(R-1)dW_4 + (C-1)\vartheta_5 dW_5, \end{aligned} \tag{3.11}$$

where

$$\begin{aligned} U\mathcal{H} = \left\{1 - \frac{1}{S}\right\}\{\Pi - \gamma LS - \beta SB - \xi SC - (\alpha_0 + v)S\} + \frac{1}{2}\vartheta_1^2 \\ + \left\{1 - \frac{1}{L}\right\}\{q(\gamma LS + \beta SB + \xi SC) - (\alpha_0 + \gamma_1)L\} + \frac{1}{2}\vartheta_2^2 \\ + \left\{1 - \frac{1}{B}\right\}\{(1-q)(\gamma LS + \beta SB + \xi SC) + p\gamma_1 L - (\alpha_0 + \alpha_1 + \gamma_2)B\} + \frac{1}{2}\vartheta_3^2 \\ + \left\{1 - \frac{1}{R}\right\}\{(1-p)\gamma_1 L + \gamma_2 B + vS - \alpha_0 R\} + \frac{1}{2}\vartheta_4^2 \\ + \left\{1 - \frac{1}{C}\right\}\{\eta_1 L + \eta_2 B - \alpha C\} + \frac{1}{2}\vartheta_5^2. \end{aligned} \tag{3.12}$$

Applying some algebraic manipulation and simplification, we arrive at

$$\begin{aligned} U\mathcal{H} \leq \Pi + 4\alpha_0 + v + \gamma_1 + \alpha_1 + \gamma_2 \\ + (\gamma + \gamma_1 + \eta_1)L + (\beta + \gamma_2 + \eta_2)B + \xi C + \alpha + \frac{1}{2}(\vartheta_1^2 + \vartheta_2^2 + \vartheta_3^2 + \vartheta_4^2 + \vartheta_5^2). \end{aligned} \tag{3.13}$$

Let $K_1 = \max\{\gamma + \gamma_1 + \eta_1, \beta + \gamma_2 + \eta_2, \xi\}$; then, by following $S + L + B + R + C \leq 1$ from Eq (3.6), the last inequality appears as follows:

$$U\mathcal{H} \leq \Pi + K_1 + 4\alpha_0 + v + \gamma_1 + \alpha_1 + \gamma_2 + \frac{1}{2}(\vartheta_1^2 + \vartheta_2^2 + \vartheta_3^2 + \vartheta_4^2 + \vartheta_5^2) := \Phi. \tag{3.14}$$

Plugging Eq (3.14) into Eq (3.11), we obtain

$$d\mathcal{H} \leq \Phi dt + (S-1)\vartheta_1 dW_1 + (L-1)\vartheta_2 dW_2 + (B-1)\vartheta_3 dW_3 + (R-1)\vartheta_4 dW_4 + (C-1)\vartheta_5 dW_5.$$

Applying the integration on both sides gives

$$\begin{aligned}\int_0^{t_\varrho\wedge T} d\mathcal{H} \leq \int_0^{t_\varrho\wedge T} \Phi dt + \int_0^{t_\varrho\wedge T} (S-1)\vartheta_1 dW_1 + \int_0^{t_\varrho\wedge T} (L-1)\vartheta_2 dW_2 \\ + \int_0^{t_\varrho\wedge T} (B-1)\vartheta_3 dW_3 + \int_0^{t_\varrho\wedge T} (R-1)\vartheta_4 dW_4 + \int_0^{t_\varrho\wedge T} (C-1)\vartheta_5 dW_5.\end{aligned} \tag{3.15}$$

The implementation of expectation yields that

$$E\Big[\mathcal{H}(S(t_\varrho\wedge T), L(t_\varrho\wedge T), B(t_\varrho\wedge T), R(t_\varrho\wedge T), C(t_\varrho\wedge T))\Big] \leq \mathcal{H}(x(0)) + E\Big[\int_0^{t_\varrho\wedge T}\Phi dt\Big],$$

which implies that

$$E\Big[\mathcal{H}(S(t_\varrho\wedge T), L(t_\varrho\wedge T), B(t_\varrho\wedge T), R(t_\varrho\wedge T))\Big] \leq \mathcal{H}(x(0)) + T\Phi. \tag{3.16}$$

Let $\Phi_\varrho = T \geq t_\varrho$ for all $\varrho \geq \varrho_1$; then, $P(\Phi_\varrho) \geq \zeta$. For every $\epsilon \in \Phi_\varrho$ there exists at least one $S(\epsilon, t_\varrho)$, $L(\epsilon, t_\varrho)$, $B(\epsilon, t_\varrho)$, $R(\epsilon, t_\varrho)$ or $C(\epsilon, t_\varrho)$ that is either equal to ϱ or $1/\varrho$, thus,

$$\mathcal{H}(S(\epsilon, t_\varrho), L(\epsilon, t_\varrho), B(\epsilon, t_\varrho), R(\epsilon, t_\varrho), C(\epsilon, t_\varrho)) \geq \Big(\frac{1}{\varrho} - 1 + \log\varrho\Big) \wedge (\varrho - \log\varrho - 1). \tag{3.17}$$

Following Eqs (3.8) and (3.16), we may write

$$\begin{aligned}\mathcal{H}(X_0) + T\Phi &\geq E\Big[1_{\Phi_{\varrho(\epsilon)}} G(S(t_\varrho\wedge T), L(t_\varrho\wedge T), B(t_\varrho\wedge T), R(t_\varrho\wedge T))\Big], \\ &= E\Big[1_{\Phi_{\varrho(\epsilon)}} G(S(t_\varrho, T), L(t_\varrho, T), B(t_\varrho, T), R(t_\varrho, T))\Big] \geq E\Big[1_{\Phi_{\varrho(\epsilon)}}\Big(\log\varrho - 1 + \frac{1}{\varrho}\Big) \\ &\quad \wedge (-\log\varrho - 1 + \varrho)\Big] = \Big(\log\varrho - 1 + \frac{1}{\varrho}\Big) \wedge (-\log\varrho - 1 + \varrho) E[1_{\Phi_{\varrho(\epsilon)}}].\end{aligned}$$

This gives that

$$\mathcal{H}(X(0)) + T\Phi \geq \zeta\Big(\log\varrho + \frac{1}{\varrho} - 1\Big) \wedge (\varrho - \log\varrho - 1).$$

In the above equation $1_{\Phi_{\varrho(\epsilon)}}$ represents the indicator function for $\Phi_\varrho(\epsilon)$. For an increase in n without bound, $\infty > \mathcal{H}(X_0) + \Phi T = \infty$ yields a contradiction; so, $t_\infty = \infty$. □

Remark 1. *The existence analysis for the considered model reveals that there exists a unique global solution $X \in \mathcal{R}_+^5$ for any initial groups of population $X(0) \in \mathcal{R}_+^5$.*

Theorem 3.3. *The proposed epidemiological model (2.1) possesses positive solutions for all initial groups of populations in $\mathcal{R}_+^5$.*

Proof. To begin the proof, we follow the work investigated in [21], and assume that $[0, +\infty)$ is the interval of solution. Since every differential equation in the model (2.1) corresponds to a geometric

Brownian motion, we assume the 5 processes to be $(\eta_S(t))_{t\in\mathcal{R}_+}$, $(\eta_L(t))_{t\in\mathcal{R}_+}$, $(\eta_B(t))_{t\in\mathcal{R}_+}$, $(\eta_R(t))_{t\in\mathcal{R}_+}$ and $(\eta_C(t))_{t\in\mathcal{R}_+}$, respectively denoted

$$
\begin{aligned}
d\eta_S(t) &= -\{\alpha_0 + v + \gamma L(t) + \beta B(t) + \xi C(t)\}\,\eta_S(t)dt + \vartheta_1\eta_S(t)dW_1(t), \quad \eta_S(0) = 1,\\
d\eta_L(t) &= \{q\gamma L(t) - (\alpha_0 + \gamma_1)\}\,\eta_L(t)dt + \vartheta_2\eta_L(t)dW_2(t), \quad \eta_L(0) = 1,\\
d\eta_B(t) &= \{(1-q)\beta S(t) - (\alpha_0 + \alpha_1 + \gamma_2)\}\,\eta_B(t)dt + \vartheta_3\eta_B(t)dW_3(t), \quad \eta_B(0) = 1,\\
d\eta_R(t) &= -\alpha_0\eta_R(t)dt + \vartheta_4\eta_R(t)dW_4(t), \quad \eta_R(0) = 1,\\
d\eta_C(t) &= -\alpha_0\eta_C(t)dt + \vartheta_4\eta_C(t)dW_5(t), \quad \eta_C(0) = 1.
\end{aligned}
$$

By applying the Itô formula to the function $\ln\eta_.$, the solution of the above system can be easily derived, as follows:

$$
\begin{aligned}
\eta_S(t) &= \exp\left[\int_0^t(\gamma L(x) + \beta B(x))dx - \left(\alpha_0 + v + \frac{\vartheta_1^2}{2}\right)t + \vartheta_1 W_1(t)\right],\\
\eta_L(t) &= \exp\left[q\beta\int_0^t S(x)dx - \left(\alpha_0 + \gamma_1 + \frac{\vartheta_2^2}{2}\right)t + \vartheta_2 W_2(t)\right],\\
\eta_B(t) &= \exp\left[(1-q)\beta\int_0^t S(x)dx - \left(\alpha_0 + \alpha_1 + \gamma_2 + \frac{\vartheta_3^2}{2}\right)t + \vartheta_3 W_3(t)\right],\\
\eta_R(t) &= \exp\left[-\left\{\alpha_0 + \frac{\vartheta_4^2}{2}\right\}t + \vartheta_4 W_4(t)\right],\\
\eta_C(t) &= \exp\left[-\left\{\alpha_0 + \frac{\vartheta_4^2}{2}\right\}t + \vartheta_5 W_5(t)\right].
\end{aligned}
$$

The solutions of the model process are derived based on the assumption that each solution can be expressed as a product of the stochastic process and associated geometric Brownian motion, i.e., $S(t) = \eta_S(t)Y_S(t)$, and $Y_S(t)$, respectively [21]. So, the stochastic integration based on the implementation of the integral to $S(t)\eta_S^{-1}(t)$ gives the assertion for $Y_S(t)$. Hence, the model solutions can be represented as follows:

$$
\begin{aligned}
S(t) &= \eta_S(t)\left\{\Pi\int_0^t \eta_S^{-1}(x)dx + S(0)\right\},\\
L(t) &= \eta_L(t)\left\{q\int_0^t \beta B(x) + \xi X(x)S(x)\eta_L^{-1}(x)dx + L(0)\right\},\\
B(t) &= \eta_B(t)\left\{B(0) + \int_0^t((1-q)(\gamma S(x) + \xi S(x) + p\gamma_1)B(u))\eta_B^{-1}(x)dx\right\},\\
R(t) &= \eta_R(t)\left\{R(0) + \int_0^t(\gamma_1(1-p)L(x) + \gamma_2 C(x) + vS(x))\eta_R^{-1}(x)dx\right\},\\
C(t) &= \eta_C(t)\left\{C(0) + \int_0^t(\eta_1 L(x) + \eta_2 C(x))\eta_C^{-1}(x)dx\right\}.
\end{aligned}
$$

Clearly, all the solutions are positive because $\eta_.$ and $\eta_.^{-1}$ are in exponential form while the initial data and all other epidemic parameters of the epidemiological model have non-negative values. □

4. Extinction and persistence of the model

In this section, we discuss the disease extinction and persistence to derive the conditions for it, which will be in the form of an expression containing white noise intensities and model epidemic parameters. Thus, the extinction of the epidemiological model (2.1) is illustrated by giving the subsequent result.

Theorem 4.1. *If*

a. $\mathcal{R}_a^S < 1$ *and* $\mathcal{R}_b^S < 1$,
b. $(1-q)(\gamma+\beta+\xi)(\alpha_0+\alpha_1+\gamma_2) \geq p(v+\alpha_0)$,

then the infection of the novel coronavirus will decay exponentially, that is

$$\limsup_{t\to\infty} \frac{\log L(t)}{t} \leq \left\{\alpha_0+\gamma_1+\frac{1}{2}\vartheta_2^2\right\}\left(\mathcal{R}_a^S-1\right) < 0,$$

and

$$\limsup_{t\to\infty} \frac{\log B(t)}{t} \leq \left\{\alpha_0+\alpha_1+\gamma_2+\frac{1}{2}\vartheta_3^2\right\}\left(\mathcal{R}_b^S-1\right) < 0.$$

In addition

$$\lim_{t\to\infty} S(t) = \frac{\Pi}{v+\alpha_0}, \quad \lim_{t\to\infty} L(t) = \lim_{t\to\infty} B(t) = \lim_{t\to\infty} C(t) = 0, \quad \lim_{t\to\infty} R(t) = \frac{v\Pi}{\alpha_0(\alpha_0+v)}.$$

Proof. To begin, we integrate both sides of the system (2.1), which gives the integral system as follows

$$\begin{aligned}
\int_0^t dS(y) &= \Pi t - \int_0^t \{\gamma L(y)+\beta B(y)+\xi C(y)+(\alpha_0+v)\}S(y)dy + \vartheta_1\int_0^t S(y)dW_1(y),\\
\int_0^t dL(x) &= \int_0^t \{q(\gamma L(y)+\beta B(y)+\xi C(y))S(y)-(\alpha_0+\gamma_1)L(y)\}dy + \vartheta_2\int_0^t L(y)dW_2(y),\\
\int_0^t dB(x) &= \int_0^t \{(1-q)\{\gamma L(y)+\beta B(y)+\xi C(y)\}S(y)+p\gamma_1 L(y)-(\alpha_0+\alpha_1+\gamma_2)C(y)\}dy\\
&\quad + \vartheta_3\int_0^t C(y)dW_3(y),\\
\int_0^t dR(y) &= \int_0^t \{(1-p)\gamma_1 L(y)+\gamma_2 C(y)+vS(y)-\alpha_0 R(y)\}dy + \vartheta_4\int_0^t R(y)dW_4(y),\\
\int_0^t dC(y) &= \int_0^t \{\eta_1 L(y)+\eta_2 C(y)-\alpha C(y)\}dy + \vartheta_5\int_0^t C(y)dW_5(y).
\end{aligned}$$

Considering the above integral system with some algebraic manipulation, we have

$$\begin{aligned}
\frac{S(t)-S(0)}{t} &= \Pi - \gamma\langle L(t)S(t)\rangle - \beta\langle B(t)S(t)\rangle - \xi\langle C(t)s(t)\rangle - (\alpha_0+v)\langle S(t)\rangle \\
&\quad + \frac{\vartheta_1}{t}\int_0^t S(y)dW_1(x), \\
\frac{L(t)-L(0)}{t} &= q\{\gamma\langle L(t)S(t)\rangle + \beta\langle B(t)S(t)\rangle + \xi\langle C(t)s(t)\rangle\} - (\alpha_0+\gamma_1)\langle L(t)\rangle \\
&\quad + \frac{\vartheta_2}{t}\int_0^t L(y)dW_2(y), \\
\frac{B(t)-B(0)}{t} &= (1-q)\{\gamma\langle L(t)S(t)\rangle + \beta\langle B(t)S(t)\rangle + \xi\langle C(t)s(t)\rangle\} + p\gamma_1\langle L(t)\rangle \\
&\quad - (\alpha_0+\alpha_1+\gamma_2)\langle B(t)\rangle + \frac{\vartheta_3}{t}\int_0^t C(y)dW_3(y), \\
\frac{R(t)-R(0)}{t} &= v\langle S(t)\rangle + \gamma_1(1-p)\langle L(t)\rangle + \gamma_2\langle C(t)\rangle - \alpha_0\langle R(t)\rangle \\
&\quad + \frac{\vartheta_4}{t}\int_0^t R(y)dW_4(y), \\
\frac{C(t)-C(0)}{t} &= \eta_1\langle L(t)\rangle + \eta_2\langle C(t)\rangle - \alpha\langle C(t)\rangle + \frac{\vartheta_5}{t}\int_0^t C(y)dW_5(y).
\end{aligned}$$

The addition of the 1st three equations gives

$$\begin{aligned}
\frac{S(t)-S(0)}{t} + \frac{L(t)-L(0)}{t} + \frac{B(t)-B(0)}{t} = & \\
\Pi - (\alpha_0+v)\langle S(t)\rangle - (\alpha_0+\gamma_1)\langle L(t)\rangle & \\
+ p\gamma_1\langle L(t)\rangle - (\alpha_0+\alpha_1+\gamma_2)\langle C(t)\rangle & \\
+ \frac{\vartheta_1}{t}\int_0^t S\,dW_1(y) + \frac{\vartheta_2}{t}\int_0^t L dW_2(y) + \frac{\vartheta_3}{t}\int_0^t C dW_3(y), & \quad (4.1)
\end{aligned}$$

which implies that

$$\langle S(t)\rangle = \frac{\Pi}{(\alpha_0+v)} - \frac{\{\alpha_0+\gamma_1(1-p)\}}{(\alpha_0+v)}\langle L(t)\rangle - \frac{(\alpha_0+\alpha_1+\gamma_2)}{(\alpha_0+v)}\langle B(t)\rangle + \Upsilon(t), \quad (4.2)$$

where

$$\begin{aligned}
\Upsilon(t) = \frac{1}{(\alpha_0+v)}\Big\{\frac{\vartheta_1}{t}\int_0^t S(y)dW_1(y) + \frac{\vartheta_2}{t}\int_0^t L(y)dW_2(y) + \frac{\vartheta_3}{t}\int_0^t B(y)dW_3(y) & \\
- \left(\frac{S(t)-S(0)}{t} + \frac{L(t)-L(0)}{t} + \frac{B(t)-B(0)}{t}\right)\Big\}. & \quad (4.3)
\end{aligned}$$

Obviously $\Upsilon(t) = 0$ as t increases without bounds to ∞

$$\lim_{t\to\infty}\Upsilon(t) = 0. \quad (4.4)$$

By the application of the Itô lemma to the model (2.1), the second equation yields

$$d\log L(t) = q\left\{\gamma S(t) + \frac{\beta S(t)B(t)}{L(t)} + \frac{\xi S(t)C(t)}{L(t)}\right\} - (\alpha_0+\gamma_1) - \frac{\vartheta_2^2}{2} + \vartheta_2 dW_2(t). \tag{4.5}$$

Integrating the above equation and then dividing both sides by t, we get the following assertion:

$$\frac{1}{t}\log L(t)|_0^t = q\left\{\gamma\langle S(t)\rangle + \beta\left\langle\frac{S(t)B(t)}{L(t)}\right\rangle + \xi\left\langle\frac{S(t)C(t)}{L(t)}\right\rangle\right\} - (\alpha_0+\gamma_1) - \frac{\vartheta_2^2}{2} + \frac{\vartheta_2 W_2(t)}{t}. \tag{4.6}$$

Since, $\left\langle\frac{S(t)B(t)}{L(t)}\right\rangle \le \langle S(t)B(t)\rangle \le \langle S(t)\rangle$ and $\left\langle\frac{S(t)C(t)}{L(t)}\right\rangle \le \langle S(t)C(t)\rangle \le \langle S(t)\rangle$, the above equation can be re-expressed follows

$$\frac{1}{t}\log L(t)|_0^t \le q\left\{(\gamma+\beta+\xi)\langle S(t)\rangle\right\} - (\alpha_0+\gamma_1) - \frac{\vartheta_2^2}{2} + \frac{\vartheta_2 W_2(t)}{t}. \tag{4.7}$$

Plugging Eq (4.2) into last equation, we arrive at

$$\begin{aligned}\frac{1}{t}\log L(t)|_0^t \le \left\{\alpha_0+\gamma+\frac{\vartheta_2^2}{2}\right\}&\left\{\frac{q(\gamma+\beta+\xi)\Pi}{(\alpha_0+v)\left(\alpha_0+\gamma_1+\frac{\vartheta_2^2}{2}\right)} - 1\right\}\\ &- \frac{q(\gamma+\beta+\xi)\{\alpha_0+(1-p)\gamma_1\}}{(\alpha_0+v)}\langle L(t)\rangle - \frac{q(\gamma+\beta+\xi)(\alpha_0+\alpha_1+\gamma_2)}{(\alpha_0+v)}\langle B(t)\rangle\\ &+ q(\gamma+\beta+\xi)\Upsilon(t) + \frac{\vartheta_2 W_2(t)}{t}.\end{aligned} \tag{4.8}$$

Using the stochastic reproductive parameters and following the *Strong Law of Large Numbers* [22], the final inequality may take the form given by

$$\limsup_{t\to\infty}\frac{\log L(t)}{t} \le \left\{\alpha_0+\gamma_1+\frac{\vartheta_2^2}{2}\right\}\left(\mathcal{R}_a^S - 1\right) < 0 \ a.s. \tag{4.9}$$

Thus, $\lim L(t) = 0$ as t increases without bound and $\mathcal{R}_1^S < 1$.

To proceed further by once again using the Itô lemma, the third equation of the epidemiological model (2.1) appears as follows:

$$\begin{aligned}d\log B(t) = (1-q)&\left\{\frac{\gamma L(t)S(t) + \beta B(t)S(t) + \xi C(t)S(t)}{B(t)}\right\}\\ &+ \frac{p\gamma_1 L(t)}{B(t)} - (\alpha_0+\alpha_1+\gamma_2) - \frac{\vartheta_3^2}{2} + \vartheta_3 dW_3(t),\end{aligned} \tag{4.10}$$

or equivalently, we can write

$$\begin{aligned}d\log B(t) \le \{\gamma S(t)L(t) + \beta B(t)S(t) + \xi C(t)S(t)\}&(1-q)\\ &+ p\gamma_1 L(t) - (\alpha_0+\alpha_1+\gamma_2) - \frac{\vartheta_3^2}{2} + \vartheta_3 dW_3(t).\end{aligned}$$

In a similar fashion as above, once again using stochastic integration, we arrive at

$$\frac{1}{t}\log B(t)|_0^t \leq (1-q)\left\{\gamma\langle L(t)S(t)\rangle + \beta\langle S(t)B(t)\rangle + \xi\langle S(t)C(t)\rangle\right\} + p\gamma_1\langle L(t)\rangle - (\alpha_0+\alpha_1+\gamma_2) - \frac{\vartheta_3^2}{2} + \frac{\vartheta_3 W_3(t)}{t}. \quad (4.11)$$

Using the same steps as performed for the previous case, the last inequality can be re-casted as follows:

$$\frac{1}{t}\log B(t)|_0^t \leq (1-q)\left\{\gamma\langle s(t)\rangle + \beta\langle s(t)\rangle + \xi\langle s(t)\rangle\right\} + p\gamma_1\langle L(t)\rangle - (\alpha_0+\alpha_1+\gamma_2) - \frac{\vartheta_3^2}{2} + \frac{\vartheta_3 W_3(t)}{t}. \quad (4.12)$$

Plugging in the value of $\langle S(t)\rangle$, Eq (4.12) can be transformed to obtain

$$\begin{aligned}\frac{1}{t}\log B(t)|_0^t \leq{}& \left\{\alpha_0+\alpha_1+\gamma_2+\frac{\vartheta_3^2}{2}\right\}\left\{\frac{(1-q)(\gamma+\beta+\xi)\Pi}{(\alpha_0+v)\left\{\alpha_0+\alpha_1+\gamma_2+\frac{\vartheta_3^2}{2}\right\}}-1\right\}\\ &-\left\{\frac{(1-q)(\gamma+\beta+\xi)\{\alpha_0+\alpha_1+\gamma_2\}}{\alpha_0+v}-p\gamma_1\right\}\langle L(t)\rangle\\ &-\frac{(1-q)(\gamma+\beta+\xi)(\alpha_0+\alpha_1+\gamma_2)}{(\alpha_0+v)}\langle B(t)\rangle\\ &+(1-q)(\gamma+\beta+\xi)\Upsilon(t)+\frac{\vartheta_3 W_3(t)}{t}. \quad (4.13)\end{aligned}$$

If $(1-q)(\gamma+\beta+\xi)(\alpha_0+\alpha_1+\gamma_2) \geq p\gamma_1(\alpha_0+v)$, then, through the use of the stochastic reproductive parameters and the implementation of the strong law of large numbers with little rearrangement and simplification, the last inequality is given by

$$\limsup_{t\to\infty}\frac{\log B(t)}{t} \leq \left\{\alpha_0+\alpha_1+\gamma_2+\frac{\vartheta_3^2}{2}\right\}\left(\mathcal{R}_b^S-1\right) < 0. \quad (4.14)$$

Hence, $\lim B(t) = 0$ as t approaches ∞ whenever $\mathcal{R}_b^S < 1$. In addition, we take the limiting system of the first, fourth, and fifth equations of the proposed model, whose solution yields that $\lim S(t) = \Pi/(\alpha_0+v)$, $\lim R(t) = \frac{v\Pi}{\alpha_0(v+\alpha_0)}$ and $\lim C(t) = 0$ if t increases without bound. Thus, the extinction is subject to the values of the stochastic reproductive parameters $\mathcal{R}_a^S$ and $\mathcal{R}_b^S$, and if they are less than unity, the disease will go extinct. □

Theorem 4.2. *For the initial groups of the population* $(S(0), L(0), B(0), R(0), C(0))$ *in* Φ*, the solutions of the epidemiological model (2.1) satisfy*

$$L_2 \leq \liminf_{t\to\infty}\langle L(t)\rangle \leq \sup\langle L(t)\rangle \leq L_1,$$

$$B_2 \leq \liminf_{t\to\infty}\langle B(t)\rangle \leq \sup\langle B(t)\rangle \leq B_1,$$

and

$$C_2 \leq \liminf_{t\to\infty} \langle C(t)\rangle \leq \sup \langle C(t)\rangle \leq C_1,$$

where

$$L_1 = \frac{(\alpha_0+v)\left\{\alpha_0+\gamma+\frac{\vartheta_2^2}{2}\right\}\left(\mathcal{R}_a^S-1\right)}{q\,(\gamma+\beta+\xi)\,\{\alpha_0+(1-p)\gamma_1\}}, \quad L_2 = \frac{(v+\alpha_0)\left\{\alpha_0+\gamma_1+\frac{\vartheta_2^2}{2}\right\}\left(\mathcal{R}_c^S-1\right)}{q\gamma\,\{\alpha_0+\gamma_1(1-p)\}},$$
$$B_1 = \frac{(\alpha_0+v)\left\{\alpha_0+\alpha_1+\gamma_2+\frac{\vartheta_3^2}{2}\right\}\left(\mathcal{R}_b^S-1\right)}{(1-q)\,(\gamma+\beta+\xi)\,(\alpha_0+\alpha_1+\gamma_2)}, \quad B_2 = \left\{\alpha_0+\alpha_1+\gamma_2+\frac{\vartheta_3^2}{2}\right\}\left(\mathcal{R}_d^S-1\right),$$
$$C_1 = \frac{\eta_1}{\alpha}L_1+\frac{\eta_2}{\alpha}B_1, \quad C_2 = \frac{\eta_1}{\alpha}L_2+\frac{\eta_2}{\alpha}B_2.$$

Proof. The direct use of Eq (4.8) ultimately gives that

$$\frac{1}{t}\log L(t)|_0^t \leq \left\{\alpha_0+\gamma+\frac{\vartheta_2^2}{2}\right\}\left\{\mathcal{R}_a^S-1\right\} - \frac{q\,(\gamma+\beta+\xi)\,\{\alpha_0+(1-p)\gamma_1\}}{(\alpha_0+v)}\langle L(t)\rangle + q\,(\gamma+\beta+\xi)\,\Upsilon(t)+\frac{\vartheta_2 W_2(t)}{t}, \quad (4.15)$$

which implies that

$$\langle L(t)\rangle \leq \frac{(\alpha_0+v)\left\{\alpha_0+\gamma+\frac{\vartheta_2^2}{2}\right\}\left(\mathcal{R}_a^S-1\right)}{q\,(\gamma+\beta+\xi)\,\{\alpha_0+(1-p)\gamma_1\}} + \frac{(\alpha_0+v)}{q\,(\gamma+\beta+\xi)\,\{\alpha_0+(1-p)\gamma_1\}}\left\{q\,(\gamma+\beta+\xi)\,\Upsilon(t)+\frac{\vartheta_2 W_2(t)}{t}-\frac{1}{t}\log L(t)|_0^t\right\}.$$

Using the sup property and applying lim as t approaches ∞, we derive the following:

$$\limsup_{t\to\infty}\langle L(t)\rangle \leq \frac{(\alpha_0+v)\left\{\alpha_0+\gamma+\frac{\vartheta_2^2}{2}\right\}\left(\mathcal{R}_a^S-1\right)}{q\,(\gamma+\beta+\xi)\,\{\alpha_0+(1-p)\gamma_1\}} = L_1. \quad (4.16)$$

Similar to Eq (4.6), we can write

$$\frac{1}{t}\log L(t)|_0^t \geq \left\{\alpha_0+\gamma_1+\frac{\vartheta_2^2}{2}\right\}\left(\mathcal{R}_c^S-1\right) - \frac{q\gamma\,\{\alpha_0+(1-p)\gamma_1\}}{(v+\alpha_0)}\langle L(t)\rangle - \frac{q\gamma\,(\alpha_0+\alpha_1+\gamma_2)}{(v+\alpha_0)}\langle B(t)\rangle + q\gamma\Upsilon(t)+\frac{\vartheta_2 W_2(t)}{t}.$$

Applying some algebraic manipulation with lim inf yields

$$\liminf_{t\to\infty}\langle L(t)\rangle \geq \frac{(v+\alpha_0)\left\{\alpha_0+\gamma_1+\frac{\vartheta_2^2}{2}\right\}\left(\mathcal{R}_c^S-1\right)}{q\gamma\,\{\alpha_0+\gamma_1(1-p)\}} = L_2. \quad (4.17)$$

Similarly, the direct use of Eq (4.13) gives that

$$\frac{1}{t}\log B(t)|_0^t \leq \left\{\alpha_0+\alpha_1+\gamma_2+\frac{\vartheta_3^2}{2}\right\}\left(\mathcal{R}_b^S-1\right) - \frac{(1-q)(\gamma+\beta+\xi)(\alpha_0+\alpha_1+\gamma_2)}{(\alpha_0+v)}\langle B(t)\rangle + (1-q)(\gamma+\beta+\xi)\Upsilon(t)+\frac{\vartheta_3 W_3(t)}{t}.$$

Re-arrangement with some algebraic manipulation yields

$$\langle B(t)\rangle \leq \frac{(\alpha_0+v)\left\{\alpha_0+\alpha_1+\gamma_2+\frac{\vartheta_3^2}{2}\right\}\left(\mathcal{R}_b^S-1\right)}{(1-q)(\gamma+\beta+\xi)(\alpha_0+\alpha_1+\gamma_2)} + \frac{(\alpha_0+v)}{(1-q)(\gamma+\beta+\xi)(\alpha_0+\alpha_1+\gamma_2)}\left\{(1-q)(\gamma+\beta+\xi)\Upsilon(t)+\frac{\vartheta_3 W_3(t)}{t}-\frac{1}{t}\log B(t)|_0^t\right\}.$$

Through the implementation of lim with sup for an increasing t without bound, the last inequality may take the following form:

$$\limsup_{t\to\infty}\langle B(t)\rangle \leq \frac{(\alpha_0+v)\left\{\alpha_0+\alpha_1+\gamma_2+\frac{\vartheta_3^2}{2}\right\}\left(\mathcal{R}_b^S-1\right)}{(1-q)(\gamma+\beta+\xi)(\alpha_0+\alpha_1+\gamma_2)} = B_1. \tag{4.18}$$

Likewise, from Eq (4.10), we obtain that

$$\frac{1}{t}\log B(t)|_0^t \geq \left\{\alpha_0+\alpha_1+\gamma_2+\frac{\vartheta_3^2}{2}\right\}\left(\mathcal{R}_d^S-1\right) - \frac{(1-q)\beta(\alpha_0+\alpha_1+\gamma_2)}{v+\alpha_0}\langle B(t)\rangle + (1-q)\beta\Upsilon(t)+\frac{\vartheta_3 W_3(t)}{t}.$$

As t approaches ∞, taking lim and inf, we can obtain the following assertion from the last inequality

$$\liminf_{t\to\infty}\langle B(t)\rangle \geq \left\{\alpha_0+\alpha_1+\gamma_2+\frac{\vartheta_3^2}{2}\right\}\left(\mathcal{R}_d^S-1\right) = B_2. \tag{4.19}$$

In addition, from the last equation of the integral system of the model (2.1), we can write

$$\langle C(t)\rangle = \frac{\eta_1}{\alpha}\langle L(t)\rangle + \frac{\eta_2}{\alpha}\langle B(t)\rangle - \frac{1}{\alpha}\left\{\frac{C(t)-C(0)}{t}-\frac{\vartheta_5}{t}\int_0^t C(y)dy\right\}.$$

By taking lim as t increases without bound and applying sup and inf respectively to the above equation, we obtain the following assertions

$$\limsup_{t\to\infty}\langle C(t)\rangle \leq \frac{\eta_1}{\alpha}L_1+\frac{\eta_2}{\alpha}B_1 = C_1, \tag{4.20}$$

and

$$\liminf_{t\to\infty}\langle C(t)\rangle \geq \frac{\eta_1}{\alpha}L_2+\frac{\eta_2}{\alpha}B_2 = C_2. \tag{4.21}$$

Thus, Eqs (4.16)–(4.21) imply that $L_2 \leq \liminf\langle L(t)\rangle \leq \limsup\langle L(t)\rangle \leq L_1$, $B_2 \leq \liminf\langle B(t)\rangle \leq \limsup\langle B(t)\rangle \leq B_1$ and $C_2 \leq \liminf\langle C(t)\rangle \leq \limsup\langle C(t)\rangle \leq C_1$, if t tends to ∞ and $\mathcal{R}_a^S > 1$, $\mathcal{R}_b^S > 1$, $\mathcal{R}_c^S > 1$ and $\mathcal{R}_d^S > 1$, which proves the conclusion. □

5. Discretization of the model and numerical experiments

To perform the numerical assessment of the stochastic epidemiological model (2.1), we chose to use the numerical Milstein higher-order method; for details, see [23]. Here, we will first demonstrate the model discretization that is used for the numerical investigation.

5.1. Discretization of the model

For, this, we assume that if $K \geq 0$ and the interval of time is $[0, T]$ with the time step $\Delta t = T/K$, then $l_i = i\Delta t$ is the point of the discretized interval. We also use $(S_i, L_i, B_i, R_i, C_i)$ while writing $(S(l_i), L(l_i), B(l_i), R(l_i), C(l_i))$ and $W_j(l_i) = W_{ji}$, $j = 1, 2, 3, 4, 5$ for simplicity. Thus, the truncation of the Itô-Taylor expansion gives the procedure of Milstein's scheme for the reported model (2.1):

$$
\begin{aligned}
S_i &= S_{i-1} + \left\{\Pi - \gamma S_{j-1}L_{i-1} - \beta S_{j-1}B_{i-1} - \xi S_{j-1}C_{i-1} - (v + \alpha_0)\right\}\Delta t \\
&\quad + \vartheta_1 S_{i-1}(W_{1_i} - W_{1_{i-1}}) + \frac{1}{2}\vartheta_1^2 S_{i-1}\left\{(W_{1_i} - W_{1_{i-1}})^2 - \Delta t\right\}, \\
L_i &= L_{i-1} + \left\{q\left(\gamma S_{j-1}L_{i-1} + \beta S_{j-1}B_{i-1} + \xi S_{j-1}C_{i-1}\right) - (\alpha_0 + \gamma_1)L_{i-1}\right\}\Delta t \\
&\quad + \vartheta_2 L_{i-1}(W_{2_i} - W_{2_{i-1}}) + \frac{1}{2}\vartheta_2^2 L_{i-1}\left\{(W_{2_i} - W_{2_{i-1}})^2 - \Delta t\right\}, \\
B_i &= B_{i-1} + \left\{(1-q)\left(\gamma S_{j-1}L_{i-1} + \beta S_{j-1}B_{i-1} + \xi S_{j-1}C_{i-1}\right) - (\alpha_0 + \alpha_1 + \gamma_2)B_{i-1}\right\}\Delta t \\
&\quad + \vartheta_3 B_{j-1}(W_{3_i} - W_{3_{i-1}}) + \frac{1}{2}\vartheta_3^2 B_{i-1}\left\{(W_{3_i} - W_{3_{i-1}})^2 - \Delta t\right\}, \\
R_i &= R_{i-1} + \{vS_{i-1} - \alpha_0 R_{i-1} + q\gamma_1 L_{i-1} + \gamma_2 B_{i-1}\}\Delta t + \vartheta_4 R_{i-1}(W_{3_i} - W_{3_{i-1}}) \\
&\quad + \frac{1}{2}\vartheta_4^2 R_{i-1}\left\{(W_{4_i} - W_{4_{i-1}})^2 - \Delta t\right\}, \\
C_i &= C_{i-1} + \{\eta_1 L_{i-1} - \alpha C_{i-1} + \eta_2 B_{i-1}\}\Delta t + \vartheta_5 C_{j-1}(W_{5_i} - W_{5_{i-1}}) \\
&\quad + \frac{1}{2}\vartheta_5^2 C_{i-1}\left\{(W_{5_i} - W_{5_{i-1}})^2 - \Delta t\right\}.
\end{aligned}
$$

To calculate the discretized Brownian paths that will be applied for $W_j(l_i) - W_j(l_{i-1})$ for the model (2.1) discretization, we assume the step size Δt to be an integral multiple of $R \geq 1$ of the increment δt. So the increments $W_j(l_i) - W_j(l_{i-1})$ becomes

$$
W_j(l_j) - W_i(l_{j-1}) = \sum_{k=i\mathcal{R}-\mathcal{R}+1}^{i\mathcal{R}} dW_k.
$$

Thus, the implementation of Milstein's higher order method for the considered model can be concluded with the following steps.

(1) Interval descretization of $[0, T]$ into subintervals $\delta t = \frac{T}{K} > 0$: $0 = l_0 < l_1 < \cdots < l_K = T$ in K with equal width with $l_n = n\delta t$.
(2) Defining the proper initial data for the compartmental population groups of the model $(S_0, L_0, B_0, R_0, C_0)$.
(3) Defining the recursive formulas $(S_j, L_j, B_j, R_j, C_j)$ for $1 \leq i \leq K$ as described through the procedure of Milstein's scheme.

(4) Discretizing the Brownian paths to be used in the calculation of $W_j(l_i) - W_j(l_{i-1})$ while using the constant $R \geq 1$ and increment Δt.
(5) Finding of $W_j(l_i) - W_j(l_{i-1}) = W_j(iR\delta t) - W_j((i-1)R\delta t) = \sum_{k=iR-R+1}^{iR} dW_k$.

5.2. Numerical experiments

We shall present the numerical experiment of the model with the aid of Milstein's Higher Order method as concluded in the above algorithm. According to Milstein's higher order method, we can assume two different sets of parameter values based on the sufficient analysis and calculations of the conditions that satisfy the derived analytical results in Theorems 4.1 and 4.2. We also assume some feasible biological initial sizes of the groups of the compartmental populations while implementing the algorithm. More precisely, the set of values of the epidemiological parameters for extinction analysis is assumed to be $A_1 = \{\Pi, \gamma, \beta, \xi, \alpha_0, v, \gamma_1, \alpha_1, \gamma_2, p, q, \eta_1, \eta_2, \alpha, \vartheta_1, \vartheta_2, \vartheta_3, \vartheta_4, \vartheta_5\}$, where the values are assigned as $\Pi = 0.9, \gamma = 0.68, \beta = 0.03, \xi = 0.1, v = 0.40, \alpha = 0.34, \vartheta_1 = 0.32, \vartheta_2 = 0.31, \vartheta_3 = 0.451, \vartheta_4 = 0.731, \vartheta_5 = 0.64, \alpha = 0.6, q = 0.51, \gamma_1 = 0.35, p = 0.022, \gamma_2 = 0.06, \alpha_1 = 0.65, \eta_1 = 0.43$ and $\eta_2 = 0.87$, while the densities for the initial data were adjusted to be $S(0) = 0.50$, $L(0) = 0.40$, $B(0) = 0.30$, $R(0) = 0.20$, $C(0) = 0.10$. Using these parametric values and initial data, we chose to implement Milstein's higher order scheme for the proposed epidemiological model (2.1) in Matlab and produce the output as depicted in Figures 2–6, which respectively demonstrate the temporal dynamics of susceptible, latent or asymptomatic and symptomatic, recovered individuals, as well as the amount of reservoir in the long term. This investigates the model extinction, which reveals that in the case of extinction analysis, the calculation of the stochastic reproductive parameters implies that $\mathcal{R}_a^S = 0.68$, $\mathcal{R}_b^S = 0.96$, $\mathcal{R}_c^S = 0.57$, and $\mathcal{R}_d^S = 0.041$, while the infected population, as well as the amount of reservoirs, goes to zero (vanishes) in the long term, as shown in Figures 3, 4 and 6. However, there will be always a non-infected population in the case of model extinction as shown in Figures 2 and 10.

On the other hand, the set A_2 is assumed to be the set of parameters whose values for the model persistence have been adjusted to be $\gamma = 0.68, \beta = 0.3, \xi = 0.1, v = 0.40, \Pi = 0.9, \alpha = 0.14, \vartheta_1 = 0.31, \vartheta_2 = 0.41, \vartheta 3 = 0.251, \vartheta_4 = 0.731, \vartheta_5 = 0.64, \alpha = 0.6, q = 0.51, \gamma_1 = 0.35, p = 0.022, \gamma_2 = 0.06, \alpha_1 = 0.65, \eta_1 = 0.43$ and $\eta_2 = 0.87$, while the initial data are same as that taken in the case of model extinction. We accordingly calculated the values of the reproductive parameters to be $\mathcal{R}_a^S = 1.59$, $\mathcal{R}_b^S = 3.80$, $\mathcal{R}_c^S = 1.00$ and $\mathcal{R}_d^S = 1.05$. With these parametric values and initial data, the implementation of Milstein's higher order algorithm generates the outputs shown in Figures 7–11, which depict the temporal dynamics of the model population whenever $\mathcal{R}_a^S > 1$, $\mathcal{R}_b^S > 1$, $\mathcal{R}_c^S > 1$ and $\mathcal{R}_d^S > 1$. We observed that in the case that the values of the reproductive numbers are greater than unity, there will always be infected individuals and an amount of reservoir in the community as shown in Figures 8, 9, and 11 respectively. Accordingly, the disease will persist and reach an endemic level. In addition, we also observed a strong impact of noise in coronavirus 2 transmission, where increasing noise intensity leads to the extinction; however, there is an inverse relation between the persistence and noise intensity.

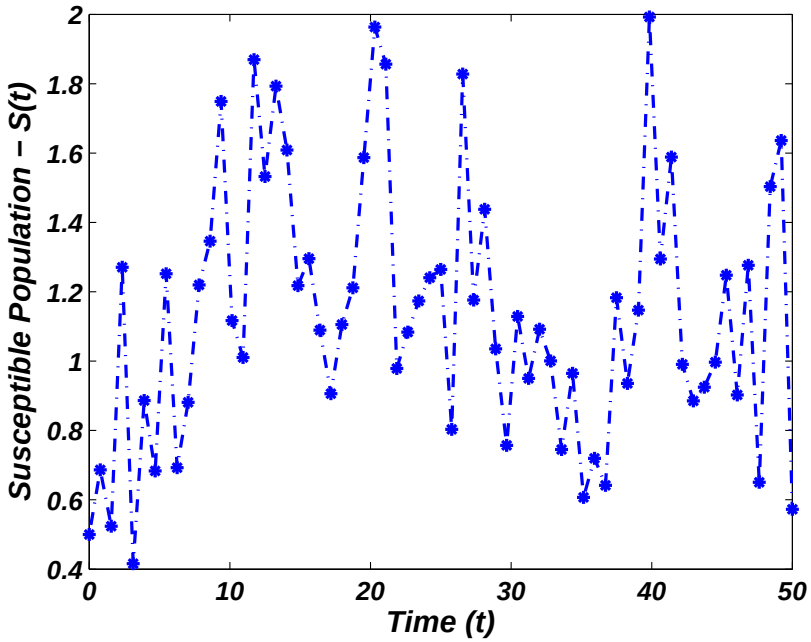

Figure 2. The plot demonstrates the dynamics of the susceptible individuals for varying parametric values given in the set A_1. This evaluates the model extinction and the existence of susceptible individuals.

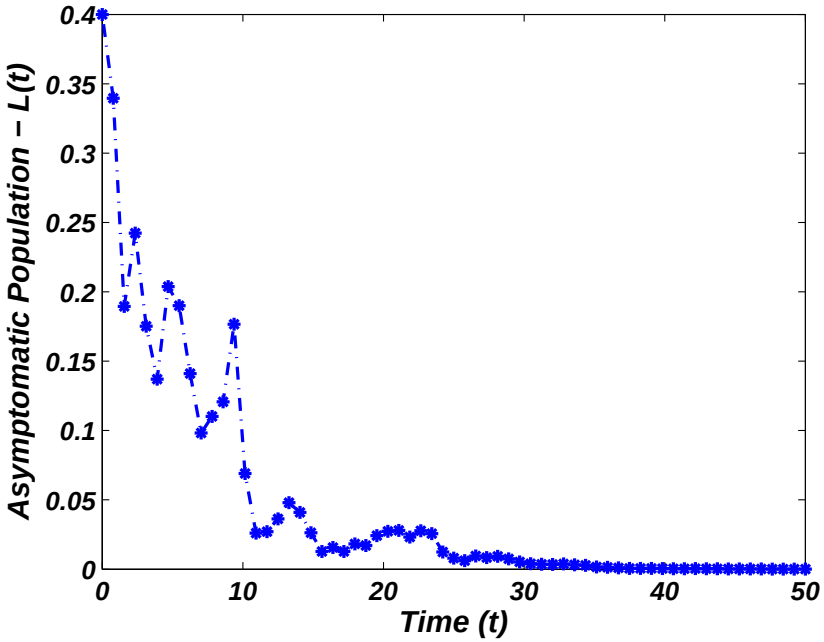

Figure 3. The dynamics of the asymptomatic/latent population of the model (2.1) for varying parametric values implemented in the set A_1, which reveals the disappearance of asymptomatic individuals with the passage of time whenever $\mathcal{R}_a^S < 1$ and $\mathcal{R}_b^S < 1$.

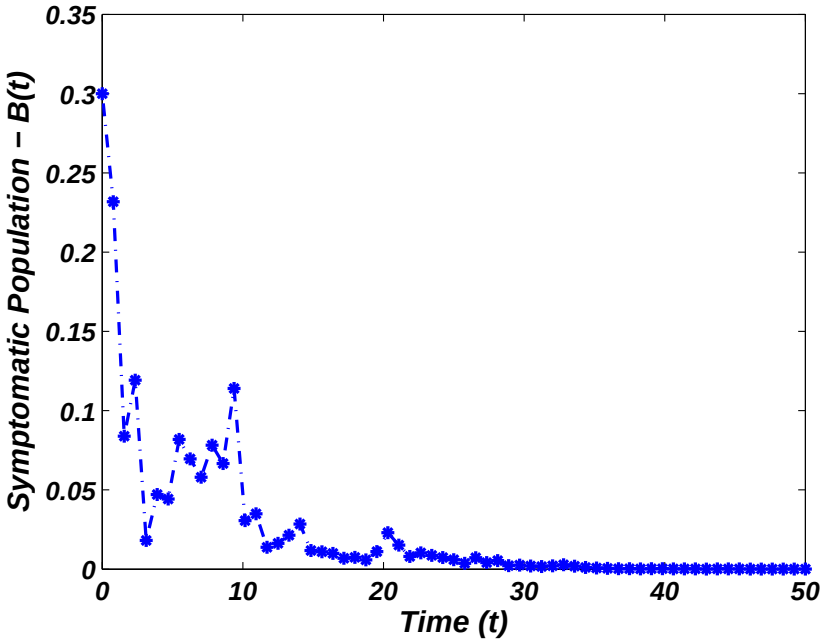

Figure 4. The temporal dynamics of symptomatic individuals of the proposed model (2.1), where the parametric values were taken from the set A_1. This reveals the extinction of the symptomatic population i.e. if $\mathcal{R}_a^S < 1$ and $\mathcal{R}_b^S < 1$, the symptomatic population goes to zero time passes.

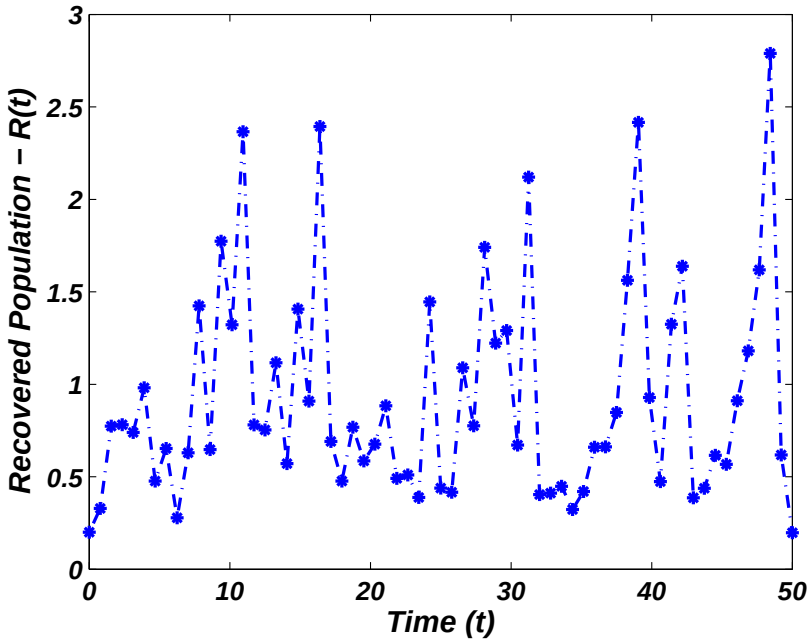

Figure 5. This shows the dynamics of the recovered individuals of the epidemiological model (2.1) for the parametric values given in the set A_1 for the investigation of model extinction. If $\mathcal{R}_a^S < 1$ and $\mathcal{R}_b^S < 1$, there will always be a recovered population.

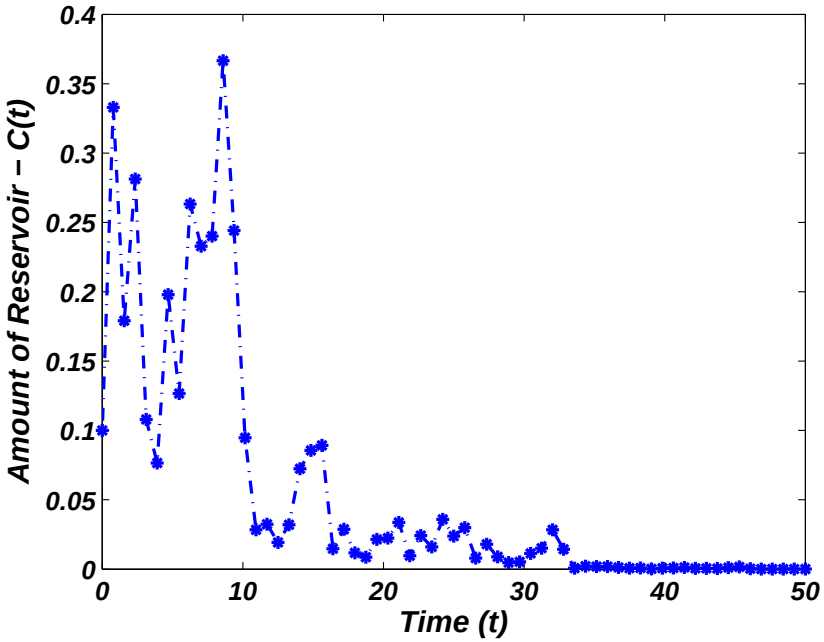

Figure 6. The dynamics of the environmental reservoir for varying epidemic parameter values described in A_1, showing that for $\mathcal{R}_a^S < 1$ and $\mathcal{R}_b^S < 1$, the amount of environmental reservoir diminishes over time.

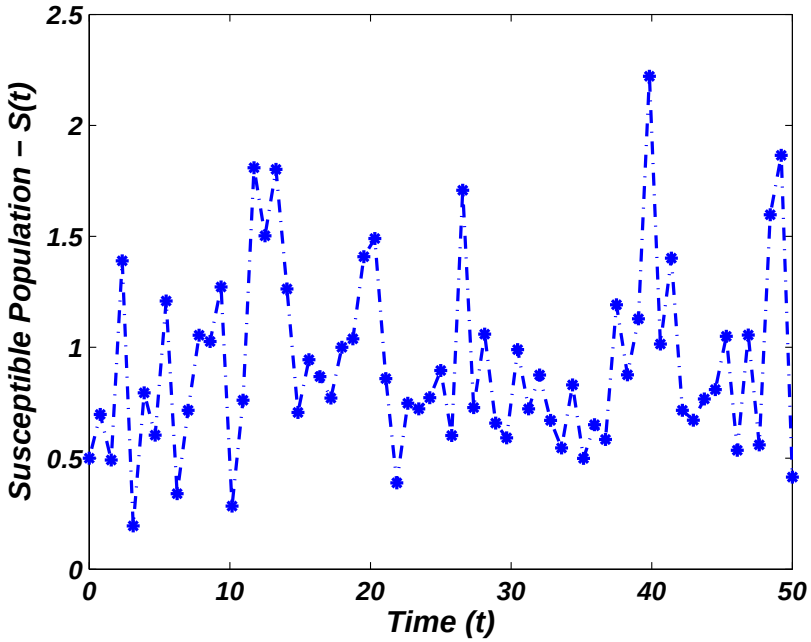

Figure 7. The temporal dynamics of the susceptible population of the model (2.1) for varying epidemic parameter values presented in A_2, showing the persistence of the novel coronavirus disease.

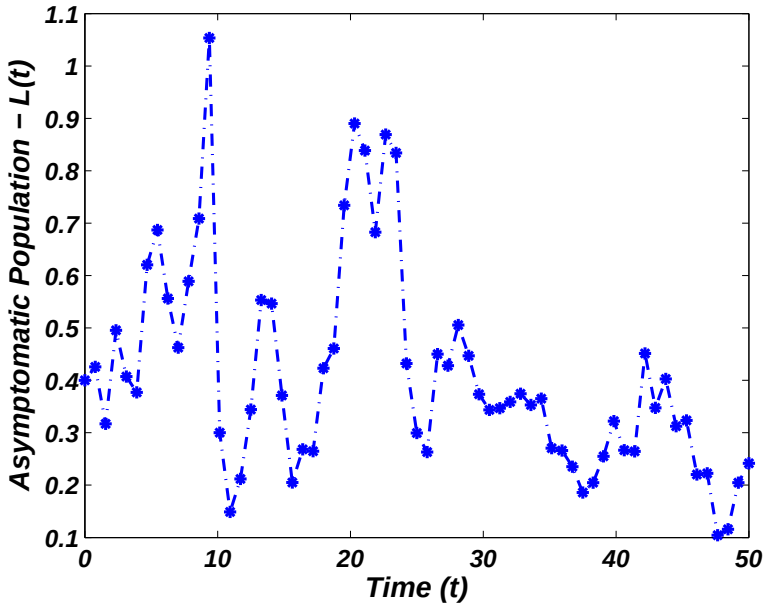

Figure 8. The dynamics of the asymptomatic population, where the parameter values were taken form the set A_2, demonstrating the persistence of the disease. This shows that, whenever $\mathcal{R}_a^S > 1$, $\mathcal{R}_b^S > 1$, $\mathcal{R}_c^S > 1$ and $\mathcal{R}_d^S > 1$, there will always be an infected population in the community.

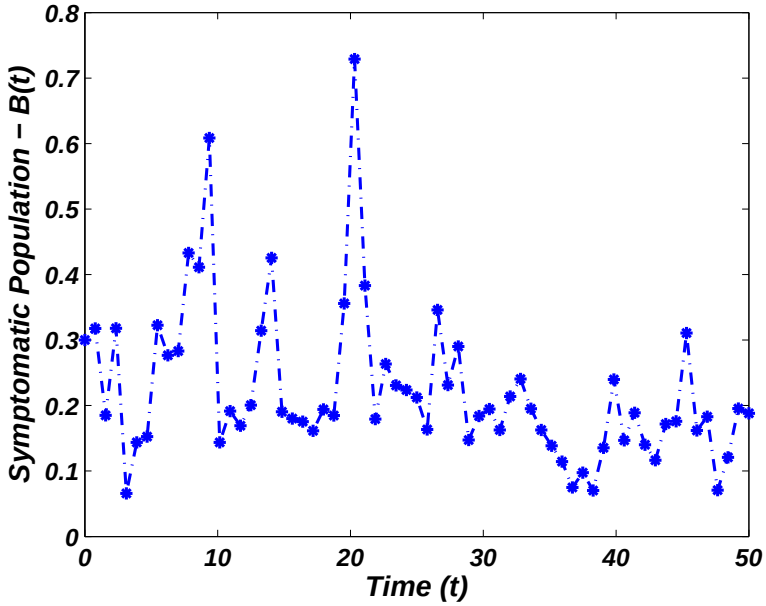

Figure 9. The plot shows the persistence of the symptomatically infected population, where the parameter values were chosen from A_2, demonstrating that for $\mathcal{R}_a^S > 1$, $\mathcal{R}_b^S > 1$, $\mathcal{R}_c^S > 1$ and $\mathcal{R}_d^S > 1$, there will always be symptomatically infected individuals in the community in the long term.

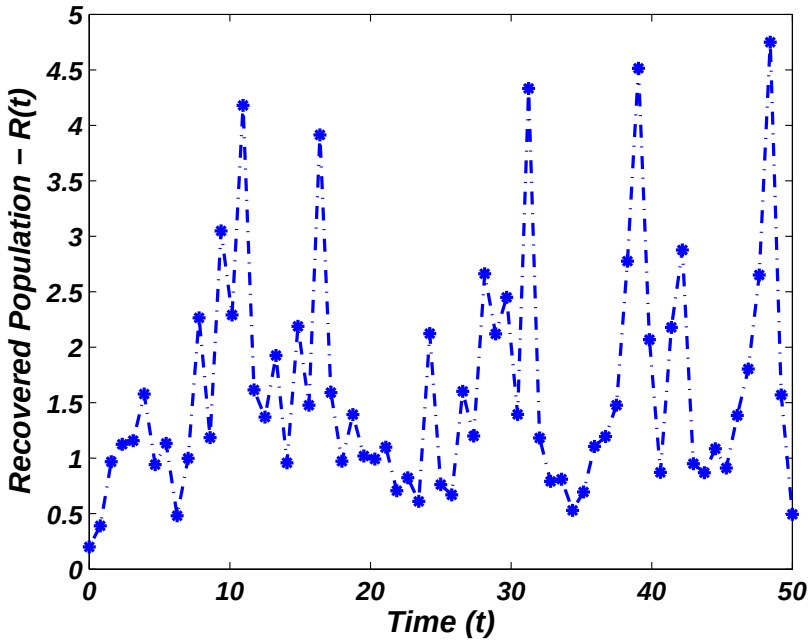

Figure 10. The dynamics of the recovered population for varying parametric values chosen from A_2, demonstrating the persistence of the compartmental population of the epidemiological model (2.1).

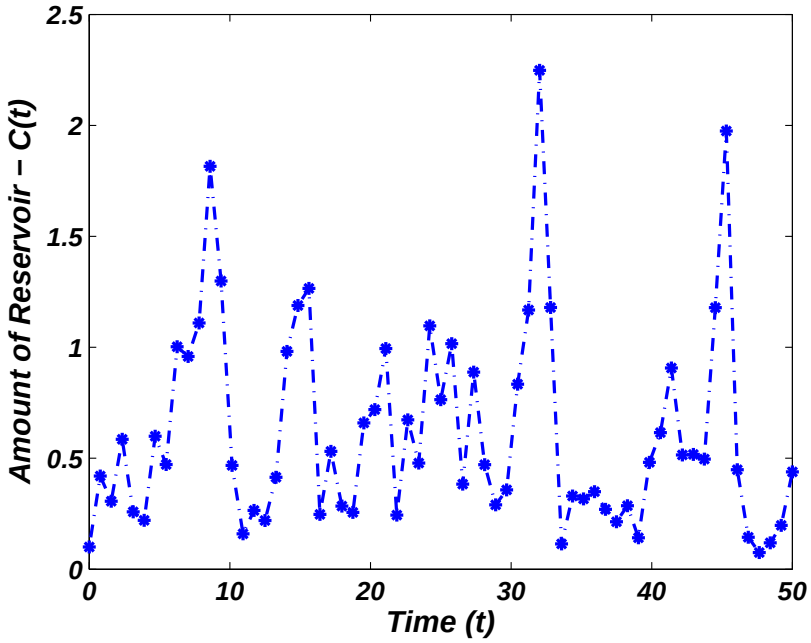

Figure 11. The visualization of the environmental reservoirs for varying values of the model parameters taken from A_2, demonstrating that there will always be the existence of environmental reservoirs in the long term whenever $\mathcal{R}_a^S > 1$, $\mathcal{R}_b^S > 1$, $\mathcal{R}_c^S > 1$, and $\mathcal{R}_d^S > 1$.

6. Conclusions

In this work, we investigated the dynamics of SARS-CoV-2 virus transmission under the effects of asymptomatic and symptomatic infection phases, and various sources of randomness by assuming variation in all groups of the model compartmental populations. Keeping in view the asymptotic behavior of the disease, we categorized the infected group of individuals into two subcategories namely, asymptomatic and symptomatic populations, as both are responsible for the transmission of the disease. More precisely, we classified the total populations, into four epidemiological groups of susceptible, asymptomatically infected, symptomatically infected, and recovered individuals, and we assumed that both the asymptomatic and symptomatic individuals are causes of diseases transmission and the production of environmental reservoirs. We also used the probability-based disease transmission coefficient because susceptible individuals either become asymptomatic or symptomatic after getting infected. The model has been developed and studied in terms of its biological and mathematical feasibility to prove that the considered problem is well-possed. We then calculated the threshold quantities and derived the conditions for the model extinction and persistence. Finally, on the basis of theoretical results, we developed the algorithm with the aid of Milstein's higher order procedure to verify the model and show the validity of the results that have been obtained in the theoretical investigation of the model. We observed that the asymptotic behavior of the infected individuals and the white noise intensity are very influential in the analysis of the dynamics of SARS-CoV-2 virus transmission. The extinction of the disease is directly related to the intensity of noise while there is an inverse relationship between persistence and the intensity of white noise.

In the future, we will incorporate suitable time dependent control measures into the proposed model by using optimal control theory to design a mechanism that leads to elimination of the infection from the community. We will also study the fractional version of the model with the aid of fractional calculus. Further, we will use the Euler-Maruyama scheme and exponential Euler-Maruyama method for simulation purposes.

Use of AI tools declaration

The authors declare that they have not used Artificial Intelligence (AI) tools in the creation of this article.

Acknowledgments

The authors would like to extend their appreciation to the Deanship of Scientific Research at King Khalid University for supporting this work through a research group program under grant no. R.G.P2/202/44. Further, the author Muhammad Bilal Riaz is thankful to the Ministry of Education, Youth and Sports of the Czech Republic for their support through the e-INFRA CZ (ID: 90254).

Conflict of interest

The authors declare no conflict of interest.

References

1. Z. Wu, J. M. McGoogan, Characteristics of and important lessons from the coronavirus disease 2019 (Covid-19) outbreak in China: Summary of a report of 72 314 cases from the chinese center for disease control and prevention, *JAMA*, **323** (2020), 1239–1242. https://doi.org/10.1001/jama.2020.2648
2. L. Ferretti, C. Wymant, M. Kendall, L. Zhao, A. Nurtay, L. Abeler-Dörner, et al., Quantifying SARS-CoV-2 transmission suggests epidemic control with digital contact tracing, *Science*, **368** (2020), eabb6936. https://doi.org/10.1126/science.abb6936
3. A. V. Kamyad, R. Akbari, A. A. Heydari, A. Heydari, Mathematical modeling of transmission dynamics and optimal control of vaccination and treatment for hepatitis B virus, *Comput. Math. Method. M.*, **2014** (2014), 475451. https://doi.org/10.1155/2014/475451
4. S. Cai, Y. Cai, X. Mao, A stochastic differential equation sis epidemic model with two correlated brownian motions, *Nonlinear Dynam.*, **97** (2019), 2175–2187. https://doi.org/10.1007/s11071-019-05114-2
5. A. Nwankwo, D. Okuonghae, A mathematical model for the population dynamics of malaria with a temperature dependent control, *Differ. Equat. Dyn. Sys.*, **30** (2022), 719–748. https://doi.org/10.1007/s12591-019-00466-y
6. A. Din, A. Khan, Y. Sabbar, Long-term bifurcation and stochastic optimal control of a triple-delayed Ebola virus model with vaccination and quarantine strategies, *Fractal Fract.*, **6** (2022), 578. https://doi.org/10.3390/fractalfract6100578
7. P. R. S. Rao, M. N. Kumar, A dynamic model for infectious diseases: the role of vaccination and treatment, *Chaos Soliton. Fract.*, **75** (2015), 34–49. https://doi.org/10.1016/j.chaos.2015.02.004
8. A. Akgül, S. H. Khoshnaw, A. S. Abdalrahman, Mathematical modeling for enzyme inhibitors with slow and fast subsystems, *Arab J. Basic Appl. Sci.*, **27** (2020), 442–449. https://doi.org/10.1080/25765299.2020.1844369
9. A. Omame, D. Okuonghae, R. Umana, S. Inyama, Analysis of a co-infection model for HPV-TB, *Appl. Math. Model.*, **77** (2020), 881–901. https://doi.org/10.1016/j.apm.2019.08.012
10. D. Li, F. Wei, X. Mao, Stationary distribution and density function of a stochastic SVIR epidemic model, *J. Franklin I.*, **359** (2022), 9422–9449. https://doi.org/10.1016/j.jfranklin.2022.09.026
11. S. Majee, S. Jana, S. Barman, T. K. Kar, Transmission dynamics of monkeypox virus with treatment and vaccination controls: A fractional order mathematical approach, *Phys. Scripta*, **98** (2023), 024002. https://doi.org/10.1088/1402-4896/acae64
12. Y. Sabbar, A. Din, D. Kiouach, Influence of fractal-fractional differentiation and independent quadratic lévy jumps on the dynamics of a general epidemic model with vaccination strategy, *Chaos Soliton. Fract.*, **171** (2023), 113434. https://doi.org/10.1016/j.chaos.2023.113434
13. X. Zhai, W. Li, F. Wei, X. Mao, Dynamics of an HIV/AIDS transmission model with protection awareness and fluctuations, *Chaos Soliton. Fract.*, **169** (2023), 113224. https://doi.org/10.1016/j.chaos.2023.113224

14. A. J. Kucharski, T. W. Russell, C. Diamond, Y. Liu, J. Edmunds, S. Funk, et al., Early dynamics of transmission and control of COVID-19: A mathematical modelling study, *Lancet Infect. Dis.*, **20** (2020), 553–558. https://doi.org/10.1016/S1473-3099(20)30144-4
15. P. Samui, J. Mondal, S. Khajanchi, A mathematical model for COVID-19 transmission dynamics with a case study of india, *Chaos Soliton. Fract.*, **140** (2020), 110173. https://doi.org/10.1016/j.chaos.2020.110173
16. F. Bozkurt, A. Yousef, D. Baleanu, J. Alzabut, A mathematical model of the evolution and spread of pathogenic coronaviruses from natural host to human host, *Chaos Soliton. Fract.*, **138** (2020), 109931. https://doi.org/10.1016/j.chaos.2020.109931
17. A. G. M. Selvam, J. Alzabut, D. A. Vianny, M. Jacintha, F. B. Yousef, Modeling and stability analysis of the spread of novel coronavirus disease COVID-19, *Int. J. Biomath.*, **14** (2021), 2150035. https://doi.org/10.1142/S1793524521500352
18. T. Khan, G. Zaman, Y. El Khatib, Modeling the dynamics of novel coronavirus (COVID-19) via stochastic epidemic model, *Results Phys.*, **24** (2021), 104004. https://doi.org/10.1016/j.rinp.2021.104004
19. C. Bender, An Itô formula for generalized functionals of a fractional brownian motion with arbitrary hurst parameter, *Stoch. Proc. Appl.*, **104** (2003), 81–106. https://doi.org/10.1016/S0304-4149(02)00212-0
20. Q. Lei, Z. Yang, Dynamical behaviors of a stochastic SIRI epidemic model, *Appl. Anal.*, **96** (2017), 2758–2770. https://doi.org/10.1080/00036811.2016.1240365
21. Y. El-Khatib, A. Hatemi-J, Option valuation and hedging in markets with a crunch, *J. Econ. Stud.*, **44** (2017). https://doi.org/10.1108/JES-04-2016-0083
22. K. Chung, *The strong law of large numbers*, The Regents of the University of California, 2008, 145–156.
23. D. J. Higham, An algorithmic introduction to numerical simulation of stochastic differential equations, *SIAM Rev.*, **43** (2001), 525–546. https://doi.org/10.1137/S0036144500378302

AIMS Press